

A Differentially Private Framework in Spatial Crowdsourcing with Historical Data Learning

Shun Zhang, Benfei Duan, Zhili Chen*, Hong Zhong and Qizhi Yu

Abstract—Spatial crowdsourcing (SC) is an increasing popular category of crowdsourcing in the era of mobile Internet and sharing economy. It requires workers to be physically present at a particular location for task fulfillment. Effective protection of location privacy is essential for workers' enthusiasm and valid task assignment. However, existing SC models with differential privacy protection usually deploy only real-time location data, and their partitioning and noise additions overlaps for grids generation. Such a way may produce large perturbations to counting queries that affect success rate of task assignment and the accuracy of allocation results. In this paper, we propose a privacy framework (R-HT) for protecting location data of workers involved in SC. We use historical data learning to perform partitioning, and import real-time data directly into the second-level grid with perturbation, which realizes parallel allocation of privacy budget and a more suitable Private Spatial Decomposition (PSD) approach. Moreover, as *geocast region* (GR) construction, we introduce some optimization strategies, including scoring function and adaptive selection of locally maximum geocast radius. A series of experimental results on real-world datasets shows that our proposed R-HT scheme attains a stable success rate of task assignment, saves obvious performance overhead and is also fit for dynamic assignment of tasks on online SC platforms.

Index Terms—Spatial crowdsourcing, differential privacy, historical data learning

1 INTRODUCTION

SPATIAL crowdsourcing (SC) is a new platform that harnesses the potential of the crowd to perform real-world tasks including collecting and analyzing environmental, social and other spatiotemporal information. SC has been applied in various domains such as smart cities, environmental sensing and journalism. However, disclosing individual locations has serious privacy implications. Many mobile users do not agree to engage in SC if their privacy is violated. Thus, ensuring location privacy is an important aspect of SC.

In the last decade, several papers have been published on location privacy in SC, see the surveys [1, 2] and papers cited there. Usually workers send their locations to a trusted *Cellular Service Provider* (CSP) which collects updates and releases a *Private Spatial Decomposition* (PSD). To determine a PSD, some methods have been adopted such as kd-tree based partitioning [3], uniform grid (UG) method [4] and adaptive grids (AG) approach [4, 5]. To et al. [6] proposed a framework for protecting location privacy of workers involved in SC. They achieved privacy protection by building PSDs based on an extended AG approach, which creates sanitized data releases using noisy real-time data at the CSP. However, since the privacy budget is sequentially divided into three parts, the relatively large scale of noise greatly affects the framework performance. In particular, the success rate of task assignment failed, at most cases, to reach

the *expected utility* (EU) as is one of the specific challenges identified therein.

Following [6], we focus on protecting privacy of worker locations in SC. We utilize historical data learning for predicting the distribution of real-time locations, and build a SC framework that protects location privacy of workers with parallel allocation of privacy budget. The grids are generated by historical data learning of locations with noisy counts in each layer using linear regression. Afterward, the real-time data are imported into grids where noise is added directly to the count of workers in each second-level cell. This realizes the separation of original data that allows to use privacy budget in parallel and essentially improves the utility efficiency of privacy budget.

The main contributions are as follows:

- (i) To avoid excessive noise additions in SC with differential privacy, we propose R-HT scheme allocating privacy budget in parallel that provides effective differentially-private protection on worker locations theoretically. To our knowledge, we are the first to propose the strategy that employs historical data learning in building (dynamic) PSD, which opens a new connection between differentially private location protection framework and machine learning methods.
- (ii) Before constructing the continuous region *GR*, we import real-time data of worker locations into the finished PSD and directly add Laplace noise to each level-2 cell. Such a separation of original data achieves a parallel composition of privacy budget which significantly reduces the impact of noise. In view of the privacy framework, our scheme improves the efficiency of system operations and ensures stably high success rate of task assignment.
- (iii) We investigate some techniques across local cell selections to fuse those cells with negative noisy counts.

- S. Zhang, B. Duan, Z. Chen and H. Zhong are with School of Computer Science and Technology, Anhui University, Hefei 230601, China
E-mail: szhang@ahu.edu.cn (S. Zhang), dbf97@stu.ahu.edu.cn (B. Duan), zlchen@ahu.edu.cn (Z. Chen), zhongh@ahu.edu.cn (H. Zhong)
- Q.Z. Yu is with Zhejiang Lab, Hangzhou 311121, China
E-mail: yuqz@zhejianglab.com
- * Corresponding author (Zhili Chen)

Manuscript received Month xx, 2020; revised Month xx, 2020.

Our selection of each newly added cell depends on a refined quality scoring function involving the area of cells, instead of its utility.

- (iv) We carry out extensive experiments on three real-world datasets which demonstrate that our R-HT scheme achieves stable success rate of task assignment and shows better performance in most aspects.

The remainder of this paper is structured as follows. In Section 2, we conduct a survey of related work. Section 3 introduces some necessary background. Section 4 describes the proposed privacy framework. Section 5 discusses the practical techniques used in our framework. Experimental results are presented in Section 6. Finally, we conclude this paper in Section 7.

2 RELATED WORK

Location Privacy Model. With the rapid development of smart mobile devices, more and more mobile applications provide location-based services, which greatly facilitates users' life. However, disclosing individual locations has serious privacy implications. Leaked locations often lead to a breach of sensitive information such as personal health, political and religious preferences. Traditional methods of location privacy protection mainly include k -anonymity, expected distance error and cryptography. Wang et al. [7] used k -anonymity method to generate $k - 1$ proper and dummy points and perform k indistinguishable queries to the service provider, using the real location and dummy locations. However, only using anonymous method can't offer good protection to a wide range of data and is vulnerable to background knowledge attack [8, 9]. Expected distance error reflects the accuracy degree to which the adversary can guess the real location by observing the obfuscated location and using available side-information [10]. Explicitly, the obfuscation mechanisms are defined by a given prior, representing the adversary's side information [11]. Cryptography is suitable for multiple parties, completely protect data privacy and prevent the leakage of data in the process of location service [12], however it normally results in high computational costs and the availability of data will decrease significantly [8]. *Differential privacy* (DP) is a new and promising privacy model, which is completely independent of attacker's background knowledge and currently a popular research topic in both academia and industry [9, 11].

Differential privacy has been proven effective in sensitive data release. Particularly, many authors have attempted to bring differential privacy into location data protection for *spatial crowdsourcing* (SC). Spatiotemporal information of workers, tasks, and intermediate results needs to be properly transformed to avoid privacy leakage while allowing efficient information processing including task assignment. There are some recent works devoted to balance between the strength of privacy protection and the efficiency of other operations in various SC scenarios. To et al. [6] divided the whole data domain into indexed units of grids (PSD) at the CSP. After receiving a task, the untrusted SC-server queries the PSD to determine a *geocast region* (GR) for task assignment. Any adversary can't identify worker's location from the published GR. However, this scheme adds noises to all

grids layer by layer, which reduces the efficiency of privacy budget and affects the performance of the framework. Xiong et al. [13] proposed a new SC model based on reward, and adopts a reward based allocation strategy to ensure the task assignment success rate. Based on geo-indistinguishability, To et al. [14] presented a framework for protecting location privacy of both workers and tasks during the tasking phase without relying on any trusted entity, in which techniques were devised to quantify the probability of reachability between a task and a worker. Wang et al. [15] proposed a novel distributed agent-based privacy-preserving framework that introduces a new level of multiple agent between users and the untrusted server and realizes the w -event ϵ -DP for real-time crowd-sourced statistical data publishing with the untrusted server. Recently, Wei et al. [16] constructed two sets of PSDs to achieve task allocation with high data utility and simultaneously protect task and worker locations.

Private Spatial Decomposition. To create sanitized data releases, PSD structures are often constructed in SC system. These partition the domain into smaller regions, and report noisy statistics on the locations within each region. A suitable PSD can often improve the success rate of task assignment and reduce system overhead. Previously, PSDs are usually based on tree, especially kd-tree and quadtree [3, 17], and the result is a deep tree. The typically simple method should be *Uniform Grid method* (UG), which treats all dense and sparse regions equally in the domain [4]. Alternatively, *Adaptive Grids approach* (AG) was proposed [4]. At the first level, AG creates a coarse-grained, equally spaced $m_1 \times m_1$ grid over the data domain. Then, each level-1 cell is partitioned into $m_2 \times m_2$ level-2 cells with m_2 chosen adaptively. This partitioning method emphasizes cell's difference in sparseness brought by UG, and it can be applied to various cases for data distributions. Later, The partition granularity was optimized with good universality in [6], and such a granularity arrangement is utilized in our proposed scheme. Gong et al. [18] proposed a partitioning method (R-PSD) based on reputation and location, where reputation is regarded as a new data dimension in building PSD by AG method and each R-PSD is composed of several sub-PSDs with different reputation levels.

In the traditional two-layer AG method, the privacy budget is divided into three parts for worker counting in the whole domain, level-1 cells and level-2 cells, respectively. It is worth noting that partitioning does not depend on the noisy counting in level-2 cells. In this paper we deploy historical data learning to perform partitioning and achieve the separation of the original (historical and real-time) data, so that the privacy budget are assigned in parallel at PSD stage and *GR* construction stages.

Prediction by Historical Data Learning. When real-time data is unavailable or difficult to obtain, researchers often use historical data instead. Indeed, using historical data to make predictions by learning methods can often generate good results reflecting the real-time case. As for location privacy protection, there are many examples of using historical locations or historical trajectories to predict real-time locations. Xu et al. [19] proposed a real-time road traffic state prediction based on ARIMA model and Kalman filter, with using historical traffic data. Liu et al. [20] predicted user's movement trajectory and position at the next moment by

collecting locations and historical check-in information on social network.

Real-time location prediction using historical data has also been extended to the field of SC. Jiang et al. [21] predicted worker positions at the next moment by analyzing their historical movement trajectory, and assigned tasks to those workers who were willing to go to or able to physically move to the position of the task on time with a high probability. On the aspect of historical data processing and location distribution on grids, To et al. [6] performed random perturbation to simulate subsequent distribution using historical positions, while only updating the counts in level-2 cells without changing AG structure. Chen et al. [22] resamples the data at regular intervals to update the counts in the fixed grid structure. However, these above methods do not use historical data to update the partitioning structure, but renew only the data in fixed grids.

In this paper, we first propose to build PSD with historical data learning based on AG method [6], then we import real-time data and add noise to each level-2 cell, which realizes the parallel allocation of privacy budget. Moreover, we develop a scoring function derived from exponential mechanism instead of the utility function, for optimizing selections of neighbor cells, which involves the factors of cell's area and distance for *GR* construction. This promotes significantly the performance in various aspects of the system.

3 PRELIMINARIES

In this section, we introduce some notations and initial definitions, and review spatial crowdsourcing, differential privacy and linear regression method.

3.1 Spatial Crowdsourcing

Spatial Crowdsourcing (SC) is a new avenue of crowdsourcing related to real-world scenarios involving physical locations, which requires workers to physically move to a particular location to perform tasks. The roles of components involved in SC are tasks, workers and the platform (mainly SC-server). The SC-server publishes or assigns the spatial task after receiving request and finally one or more workers accept and finish the task. Usually there are two categories of task assignment modes based on how workers are matched to tasks in SC [23]. In the *Worker Selected Tasks* (WST) mode, SC-server is only responsible for the release of tasks, and workers autonomously select suitable tasks according to their own locations, without reporting the location to SC-server. In *Server Assigned Tasks* (SAT) mode, SC-server collects worker locations and runs a complex optimization matching algorithm to assign the task to one or more workers, who decide whether to accept the task or not.

The quality of spatial tasks in SC is the main criterion to determine whether the tasks are assigned effectively[2]. It is usually evaluated by reliability, which is formalized as the probability that over 50 percent of workers correctly answer the task [24], or the chance that at least one worker completes the task successfully [25]. The former is generally used for spatial tasks that require qualified answers, such as spatial data collection related to pictures and videos. For

such spatial tasks, the main challenge for SC is how to verify the validity of the results provided by untrusted workers. Since malicious workers/users may upload some incorrect information, the number of tasks correctly completed needs to be maximized [24]. The latter is generally used in the case that a spatial task needs to be completed by a single worker, such as taxi calling service and fast food delivery. In such situations, due to the factors, the worker-task distance and task expiration time, at least one assigned worker can correctly finish the task [25]. Similarly, the framework proposed by To [6] can not guarantee that the task are disseminated to enough workers, since the SC-server can only assign tasks by the sanitized PSD. Then the method of effectiveness evaluation is to compute the probability that among those assigned to the task at least one worker is willing to accept the task.

3.2 Differential Privacy

Differential privacy (DP) has emerged as the *de facto* standard privacy notion for privacy-preservation research on data analysis and publishing. It makes that the probability of any output is equally likely from all nearly identical input datasets, so that it is unable to infer any sensitive information of an individual. Afterwards, any adversary cannot conclude with high confidence whether a particular individual is involved in the query result or not.

For applying DP, a crucial choice is the condition under which the datasets D and D' are considered to be neighboring. The notion of *Unbounded DP* is used in our framework, which means that two datasets D and D' are neighboring if D can be obtained from D' by adding or removing one element.

Definition 1 (ϵ -DP [26]). *Given any two neighboring datasets D and D' , for any set of outcomes Ω , a randomized mechanism M gives ϵ -DP if the probability distribution of the mechanism output on D and D' is bounded by:*

$$\frac{\Pr(M(D) \in \Omega)}{\Pr(M(D') \in \Omega)} \leq e^\epsilon. \quad (1)$$

The parameter ϵ is termed privacy budget that is specified by a data owner and represents the privacy level to be achieved. A lower privacy budget implies a higher privacy level.

Definition 2 (Global Sensitivity [27]). *Let D and D' denote any pair of neighboring datasets. The global sensitivity of a function f , denoted by Δf , is given as below,*

$$\Delta f = \max_{D, D'} \|f(D) - f(D')\|, \quad (2)$$

which represents the maximal change on the output of f when deleting any record in D

Definition 3 (Laplace Mechanism [26]). *Given a function $f : D \rightarrow \mathbb{R}$, Δf is the sensitivity of f . The mechanism is given by*

$$M(D) = f(D) + \text{Laplace}\left(\frac{\Delta f}{\epsilon}\right) \quad (3)$$

The Laplace mechanism provides the ϵ -DP [28]. The following important properties are related to composition of algorithms for preserving ϵ -DP.

Theorem 1 (Sequential Composition [28]). M_1, M_2, \dots, M_m is a set of mechanisms, where M_i provides ϵ_i -DP. Let M be a mechanism that executes $M_1(D), M_2(D), \dots, M_m(D)$ using independent randomness for each M_i , and returns the vector of the outputs of these mechanisms. Then, M satisfies $(\sum_{i=1}^m \epsilon_i)$ -DP.

Theorem 2 (Parallel Composition [28]). Let M_1, M_2, \dots, M_m be m mechanisms that satisfy ϵ_1 -DP, ϵ_2 -DP, \dots , ϵ_m -DP, respectively. For a deterministic partitioning function f , let D_1, D_2, \dots, D_m be respectively the resulting partitions of executing f on dataset D . Publishing the results of $M_1(D_1), M_2(D_2), \dots, M_m(D_m)$ satisfies $(\max\{\epsilon_1, \epsilon_2, \dots, \epsilon_m\})$ -DP.

Theorem 3 (Post-Processing [27]). Given a randomized mechanism M_1 that satisfies ϵ -DP, then for any possibly algorithm M_2 , the composition $M_2(M_1)$ still satisfies ϵ -DP.

3.3 Linear Regression

In our setting, we add noise to the counting of the historical locations layer by layer, and use the linear regression method to predict the real-time count of workers in each cell, so as to determine (local) partitioning of the next level.

Linear regression is one of the basic learning methods in machine learning. The goal is to find a line, a plane, or even a higher-dimensional hyperplane that minimizes the error between the predicted and actual values. There are univariate and multiple linear regressions. Univariate linear regression means that only one factor is considered and the solution involves a linear equation. We use unitary regression method to predict location counts.

We evaluate some schemes with three datasets, see the details in Section 6.1. Valid historical locations of the previous 20 periods with noises in counting are used to predict the real-time distribution. Figure 1 shows the comparison between the actual counts of level-1 cells and the predicted counts with noise (with sensitivity 1 and privacy budget 0.04) added to the total count in each period on NYTaxi and Gowalla datasets, respectively. The average error rate γ is calculated by,

$$\gamma = \frac{\bar{E}}{\bar{A}}, \text{ with } \bar{E} = \frac{1}{n} \sum_{i=1}^n |P_i - A_i|, \quad (4)$$

where n represents the count of level-1 cells, \bar{A} represents the actual average count of workers of level-1 cells, P_i and A_i represent the predicted and actual counts of workers in the i -th level-1 cells, respectively. The rates γ of NYTaxi and Gowalla are 25.4% and 28.4%, respectively. This shows that in the case of very low privacy budget, the noise interference is much, the predicted result still reflect roughly the distribution of actual data, and the predicted distribution of workers can be regarded as the actual distribution.

3.4 Problem Statement

Existing SC models with differential privacy protection mainly harness real-time location data and generate PSD by performing noise additions and domain partitioning in a crossed way. They have to add sequential noise to worker counts in grids at all levels, which tends to incur relatively

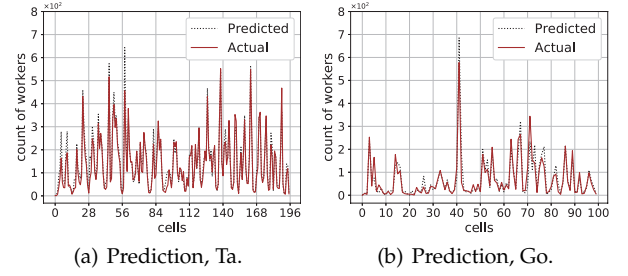


Fig. 1: Predicted and actual distribution of locations in the first-level cells

high error on many aspects and affects efficiency of SC system.

In order to improve system performance of SC with differential privacy protection, we are intended to study a new SC model. That is, given historical and real-time data of worker locations, and a privacy budget ϵ , perturb their counts with noise in parallel, generate a suitable PSD and then design a more efficient SC model with privacy protection. Specifically, with respect to parallel composition of adding noises, through the distribution of real-time positions predicted by the noisy historical data, a domain partitioning is performed without using real-time data. On the other hand, based on the grids determined previously, real-time data are directly imported into the bottom cells in which counts of the data points are perturbed with only one round. In addition, how to optimize task assignments in SC from various perspectives (particularly to achieve stable success rate of task assignment) based on PSD with perturbation is also considered in this paper.

4 BASIC FRAMEWORK

In this paper the study of privacy framework is based on the notion of unbounded DP. Then the sensitivity of workers' count in each grid (or region) is 1, that is, while the maximum increase or decrease is 1 for the total number of workers, such a change may occur in any cell [28]. Compared with unbounded DP, the sensitivity in bounded DP case is 2, the increase of noise scale will significantly affect the success rate of task assignment. This section mainly introduces the basic framework of the newly proposed privacy protection scheme, including system model, domain partitioning method, cell selection strategy in GR , and goals of system design.

4.1 System Model

Following [6], we consider the privacy protection problem of SC worker locations in the SAT mode. Fig. 2 describes our proposed system framework that consists of four parts: CSP, SC-server, requesters and workers. Workers send their real location information to CSP. As a trusted third party, CSP collects locations reported by workers, and construct PSD with noises. Requesters submits tasks and exposed location information to SC-Server. After receiving a task request, the untrusted SC-server determines GR by querying the PSD and initiates a geocast communication process. The

possible disclosure of worker location and identity posterior to consent is outside our scope.

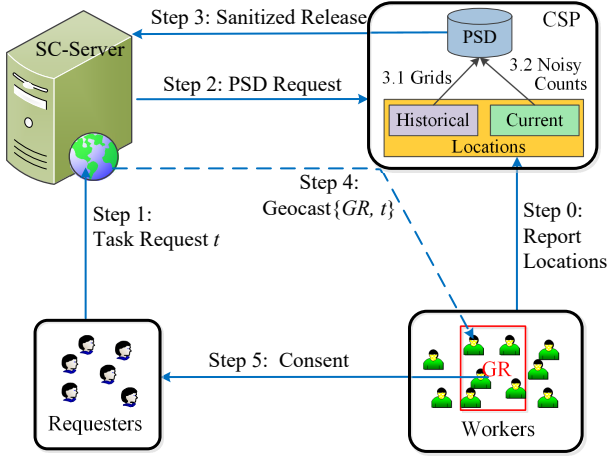


Fig. 2: Privacy framework for spatial crowdsourcing

The scheme consists of the following stages.

- Step 0: Workers report their real locations to the CSP, which will be divided into real-time and historical data.
- Step 1: A requester sends task t to SC-server.
- Step 2: SC-server queries the PSD with the CSP.
- Step 3: According to the given privacy budget ϵ , CSP partitions the data domain by using historical locations reported by workers and imports noisy real-time counts into the generated grids to update the PSD for answering to SC-server.
- Step 4: SC-server determines GR and initiates a geocast communication process in two ways (infrastructure-based or infrastructure-less mode) as in [6].
- Step 5: If a worker in GR accepts the task, she sends a consent message to the SC-server (or the requester) for confirming her availability.

The above scheme is mainly designed for a single-task assignment system model in dynamic scenarios where for each real-time task request, the CSP collects properly the latest real-time location data of workers and updates the grid structure and PSD with newly confirmed historical data, and only a worker is required to complete the task. In the static scenario, SC-server deploys a fixed PSD in a period to release GR , and Steps 0, 2 and 3 can be skipped. In the case of multiple tasks, our system model is still valid under the assumption that the task assignments do not interfere with each other.

4.2 Building PSD with Prediction

The first stage in our framework consists of building a PSD (at the CSP part), which determines the accuracy of released data and also performance metrics. Here we use the extended *Adaptive Grid method* (AG) developed in [6] together with historical locations learning. Table 1 summarizes the notations used in our description.

AG (As shown in Figure 3) reduces the non-uniformity error brought by UG by conducting two-level partition on the basis of UG. But unlike AG proposed in [6], we use

TABLE 1: Summary of Notations

Symbol	Definition
ϵ	Total privacy budget
N_p	Total number of workers by prediction
N_p^{ij}	Number of workers by prediction in the i -th row and j -th
m_1	The first level grid granularity
m_2^{ij}	Second-level partitioning granularity of i -th row
β	Budget allocation parameters for forecasting, $\beta = 0.04$
ϵ'	Parameters for grid partitioning in [6], $\epsilon' = 0.5\epsilon$

prediction by historical noisy data. The historical data set is denoted as $H = \{h_1, h_2, \dots, h_n\}$ (h_k represents the data of the k -th time period, $1 \leq k \leq n$), the whole count of locations of h_k is denoted as \tilde{N}_k . Adding Laplace noise to each \tilde{N}_k with privacy budget $\epsilon_1 = \beta\epsilon$ and getting the result \tilde{N}'_k . Establishing a linear regression model of $\tilde{N}'_1 \sim \tilde{N}'_n$ to predict the value of \tilde{N}'_{n+1} , that is, the predicted value N_p ($N_p = \tilde{N}'_{n+1}$) of the total number of real-time positions. Then calculating m_1 according to Eq. (5).

$$m_1 = \max \left(10, \left\lceil \frac{1}{4} \sqrt{\frac{N_p \times \epsilon}{k_1}} \right\rceil \right) \quad (5)$$

ϵ is the total privacy budget, which is used here as a parameter for grids partition and does not mean anything. $k_1 = 10$ according to [6].

Partitioning each h_k to $m_1 \times m_1$ cells, the set of grids of h_k is denoted as $\tilde{S}_k = \{\tilde{s}_k^{ij} \mid 1 \leq i \leq m_1, 1 \leq j \leq m_1\}$, \tilde{s}_k^{ij} represents the level-1 cell numbered ij in h_k , its number of locations is denoted as \tilde{N}_k^{ij} . For each \tilde{s}_k^{ij} in each \tilde{S}_k , adding Laplace noise with privacy budget $\epsilon_2 = \epsilon \times (1 - \beta)$ to \tilde{N}_k^{ij} and then normalizing it with rate N_p / \tilde{N}'_k , getting the result $\tilde{N}_k^{ij'}$. Establishing a linear regression model of $\tilde{N}_1^{ij'} \sim \tilde{N}_n^{ij'}$ to predict the value of $\tilde{N}_{n+1}^{ij'}$, that is the predicted value of the real-time number of locations in level-1 cell numbered ij , and then normalizing it with rate $N_p / \tilde{N}_{n+1}^{ij'}$, getting the result \tilde{N}_p^{ij} . Calculating each m_2^{ij} according to each \tilde{N}_p^{ij} by Eq.(6), the set of result is $m_2 = \{m_2^{ij} \mid 1 \leq i \leq m_1, 1 \leq j \leq m_1\}$.

$$m_2^{ij} = \left\lceil \sqrt{\frac{N_p^{ij} \times \epsilon'}{k_2}} \right\rceil \quad (6)$$

$k_2 = \sqrt{2}$ according to [6]. ϵ' is a parameter independent of the privacy budget, and we continue to use its value in [6] here ($\epsilon' = 0.5 \times \epsilon$).

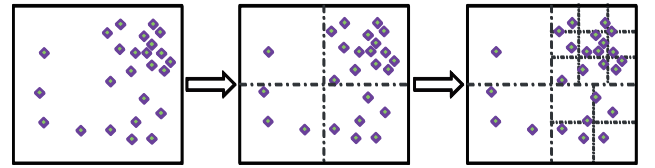


Fig. 3: AG of workspace

4.3 Geocast Region Construction

In this section, we mainly introduce the construction idea of GR . We investigate some techniques across local cell

selections to fuse those cells with negative noisy counts and use scoring function involving the area of cells instead of utility function when selecting a new cell.

For convenience, we just consider the static location of the task for now. The probability of a worker accepting a task is only related to the distance between the worker and the task. We refer to the *mean contribution distance* (*MCD*) proposed in [29], and the calculation formula of *MCD* is as follows:

$$MCD(w_i) = \sum_{j=1}^n \frac{d(L_{w_i}, L_{c_j})}{n} \quad (7)$$

Where L_{w_i} is the location of worker w_i , and L_{c_j} are the locations of its n contributions. Then according to article [30], we can consider 90% of *MCD* as *maximum travel distance* (*MTD*). *MTD* is the maximum distance a worker is willing to travel to accept a task.

Different from the utility function, the scoring function not only takes the number of workers and the cell-task distance into account, but also the cell's area. The experiment in Section 5.1 shows that the utility of the scoring function is significant. When adding a new cell to the *GR*, the score for each candidate cell needs to be calculated. The score q_t^k of the candidate cell $k \in Q$ for task t is defined as:

$$q_t^k = \frac{N_k}{f_s(S_k) \cdot f_d(D_t^k)} \quad (8)$$

where N_k represents the number of noisy workers in the candidate cell k , S_k represents the area of cell k , and D_t^k is the cell-task distance represented by the average distance between the task and four corners of cell k . It is reasonable that the higher density of workers N_k/S_k in cell k , or the shorter the cell-task distance D_t^k , the higher score q_t^k . The functions f_s and f_d are positive monotonic functions of S_k and D_t^k , respectively, which are used to control the influence strength of area and distance.

The algorithm to construct *GR* is shown in Algorithm 1.

In Line 2, in order to improve the compactness of the *GR* and avoid excessive neglect of nearby workers, we set the *Local Maximum Geocast Radius* (*LGR*) during cell selection, the calculation method of *LGR* will be covered in detail in Section 5.2. In Line 11, we add a loop termination condition that returns directly to *GR* when all candidate cells are non-positive, which will cover in detail in Section 5.3. In Line 4 and 14 we need calculated the utility value of the cell c .

$$U_t^c = 1 - (1 - AR_t^c)^{N_c} \quad (9)$$

N_c represents the noisy count of workers in c . AR_t^c represents the average task acceptance probability of the workers in cell c . $(1 - AR_t^c)^{N_c}$ represents the probability that no workers in c are willing to accept the task t . the practical meaning of U_t^c is the probability that at least one worker in cell c is willing to accept task t . All possible candidate workers for each task are limited to the *MTD* distance from the task. The AR value is generated according to the linear law of distance. The smaller the worker-task distance, the closer their AR value is to *MAR*. Once the worker-task distance reaches *MTD*, the AR is considered to be equal to 0. AR_t^c is shown in Eq. (10). (Since the workers are close

Algorithm 1 R-HT Algorithm

Input: maximum travel distance *MTD*, expected utility *EU*, task t

Output: Geocast region *GR*

- 1: Init $GR = \{\}, Q = \{\}, U = 0$
 - 2: Compute Local Maximum Geocast Radius *R* with Algorithm 2
 - 3: $GR = GR \cup c_t$, c_t is the level-2 cell that covers t
 - 4: Compute c_t 's utility U_t^c by Eq. (9)
 - 5: If $U_t^c > 0$ then $U = U_t^c$
 - 6: **while** $U \leq EU$ **do**
 - 7: Find $neighbors = \{\{c_t's\ neighbors\} - GR\} \cap MTD \cap R$
 - 8: $Q = Q \cup neighbors$
 - 9: If Q is null, return *GR*
 - 10: Find the cell c with the highest score s in Q
 - 11: If $s \leq 0$, return *GR*
 - 12: Remove c from Q
 - 13: $GR = GR \cup c$
 - 14: Compute c 's utility U_t^c by Eq. (9)
 - 15: Update U by Eq. (11)
 - 16: **end while**
-

to each other in the same cell, we set their AR to be the same).

$$AR_t^c = (1 - d/MTD) \cdot MAR \quad (10)$$

d represents the average distance between the task t and the four corners of the cell c , and *MAR* represents the maximum task acceptance rate of workers.

In Line 15, after adding c to *GR*, we first calculated grid utility according to Eq. (9), and then updated regional utility according to Eq. (11).

$$U = 1 - (1 - U)(1 - U_t^c) \quad (11)$$

When U reaches the expected utility *EU*, it returns *GR* directly, otherwise, continue to select a next new connected cell. To ensure the *GR* is a continuous region, we require that each new cell added must maintain connectivity with previous *GR*. Specifically, when adding c to *GR*, the newly added cell in Q must be the neighbor cell of c .

4.4 Design Goals

Adding noise to protect the workers' locations in SC will inevitably reduce the effectiveness of worker task matching and efficiency of task assignment. Due to the randomness of Laplace noise, the composition of *GR* will show some random and irregular changes, and even cause the distance of workers to be far away. In order to evaluate the system overhead and performance of the framework, the main evaluation indexes proposed by [6] are used:

- (1) **Assignment Success Rate (ASR).** As the noise of privacy protection mechanism leads to the uncertainty of the task release area, the number of actual workers in the area may not enough or far away from task, affecting the success rate of task assignment. In theory, ASR measures the ratio of tasks assigned successfully to the total number of task requests. The challenge we

faced was that ASR reaches the threshold EU in the average sense of several task assignments.

- (2) **Worker Travel Distance (WTD).** According to the framework setting, SC-server doesn't know the actual worker-task distance, a large distance will inevitably affect the efficiency of task execution. The goal is to keep the actual worker-task distance as small as possible on average.
- (3) **Average Number of Notified Workers (ANW).** ANW affects both the communication overhead of the GR and the computation overhead of the matching algorithm. Its goal is to inform as few workers as possible without compromising the ASR.
- (4) **the Number of Routers Required to Broadcast the GR (HOP).** In practice, task notifications to workers in the GR are sent hop-by-hop wirelessly via a router. HOP is defined as the hop count required to disseminate the task request to all workers. We approximate HOP as diameter of the GR divided by the diameter of the communication range (100 m for WiFi).
- (5) **Digital Compactness Measurement (DCM).** Based on the assumption that the communication cost is proportional to the minimum bounding circle covering GR , the ratio of the area of GR to the minimum circumferential circle area is adopted to measure the compactness of GR . Generally, the high compactness of the GR is conducive to reducing communication costs. The challenge is to get DCM as close to 1 as possible.

5 SKILL AND ANALYSIS

In this section, we introduce three practical grid selection strategies involved in the new R-HT scheme in detail and give the DP theory analysis of the whole system framework.

5.1 Cell Selection by Quality Scoring

The goal of our scheme is to reduce communication cost as little as possible and improve the success rate of task assignment when constructing GR for a single task, which requires considering the cell's selection principle when adding to GR . The utility function, which take the worker's count and cell-task distance into consideration, is usually used in the past schemes, such as G-GR. It selects the cell with the maximum utility in each step to make the number of cells in GR be the smallest. But in a grid structure that goes through two level partition, the difference of workers' count in each cell is often small. For the neighbouring level-2 cells, cell-task distance is closer to each other, but the gap on area often has dozens of times, while the utility function ignores the influence of the area, which will inevitably increase the communication overhead. For this reason, we propose to use the scoring function derived from the exponential mechanism which comprehensively takes the factors of the workers' count, cell-task distance and area into account instead of the utility function. We compare the two functions on Yelp (Ye.). The results are shown in Figure 4.

From the perspective of the scoring function versus the utility function, when constructing the scheme based on real-time data, experimental comparison shows that the G-GS using the scoring function is better than the G-GR

using the utility function, and improved 3.1%, 1.1%, 1.2%, and 3.0% on the WTD, HOP, ANW and DCM, respectively. However, there was no improvement in ASR. Therefore, we construct new schemes with historical data learning, G-HS and G-HU had 4.0% improvement in ASR. The G-HS using the scoring function still maintains above advantages in the above four indexes, because it is more preferred to choose a small grid with higher population density with considering the factor of area. The above analysis fully reflects the advantages of scoring function strategy.

From the perspective of using historical data, it can be seen from the comparison of G-HS and G-GS and the comparison of G-HU and G-GR that G-HS and G-HU (both partitioning with historical data) have higher ASR than EU , and most of them failed to meet EU when using real-time data. This is because the negative noise will reduce the workers' count (the cell's utility is 0 when the noisy count is less than 0). In the GR construction stage, the cell with a higher noisy count will be preferred which makes more positive noisy cells into GR in probability, resulting in a large number of positive virtual values. So the noisy utility of GR is generally higher than the real. In other words, when the calculated noisy U reaches EU , the real U may not reach EU . When using historical data learning, the parallel use of privacy budget makes the noise scale smaller, the deviation between calculated U and real U is smaller, so the ASR is higher. Due to this, from the comparison between G-HS_Ad (adjust the EU of G-HS point by point so that its ASR value is close to G-GS) and G-GS in the figure, it can be seen that using historical data is 3.8%, 6.7%, 3.9% and 4.4% better than using real data in the average sense of WTD, HOP, ANW and DCM.

5.2 Local Maximum Geocast Region

In order to improve the compactness of GR and avoid excessive neglect of nearby workers, we adaptively set a local maximum geocast radius R by searching when selecting cells. We consider all cells in the R as a whole, calculate the average distance by weighting the absolute value of the noisy count, and then calculate the utility of the area approximately. The initial value of R is the average distance from the task to the four corners of the cell where the task is located, and it is gradually increased according to half the width of the smallest cell in whole domain until the approximate utility reaches EU . The algorithm for finding LGR is shown in Algorithm 2.

We compared and analyzed the effects before and after adding LGR in NYTaxi(Ta.), and the results are show in Figure 5.

From the comparison of R-HS and G-HS and the comparison of R-GS and G-GS in Figure 5, we can observe that the addition of R did not excessively reduce the ASR. However, it effectively reduced other indexes, especially optimized 19.2% and 13.9% (WTD), 4.9% and 3.5% (HOP), 4.2% and 5.0% (ANW), 19.6% and 12.3% (DCM) at the privacy budget of 1.0. After adjusting the EU to make the ASR of the four schemes approximately the same, the advantages of the R-HS are more prominent. In the above all indexes, the R-HS is always the best. Compared with R-GS, R-HS is 5.2%, 5.6%, 5.9% and 1.6% better on the above indexes. In Section 6, a

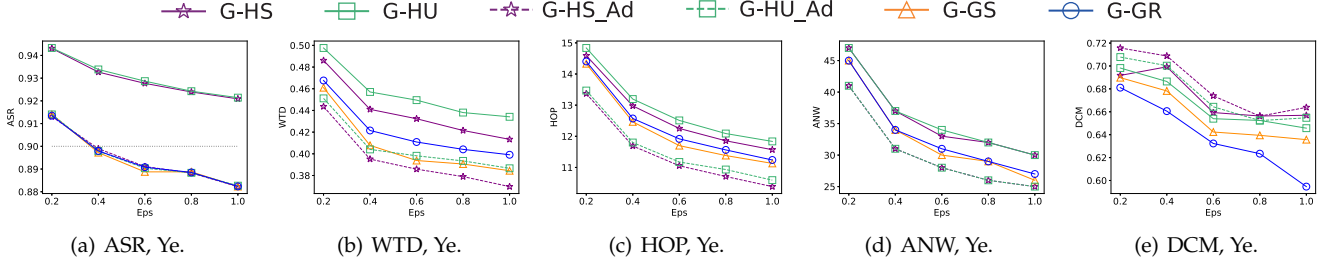


Fig. 4: The influence of the scoring function on the scheme performance

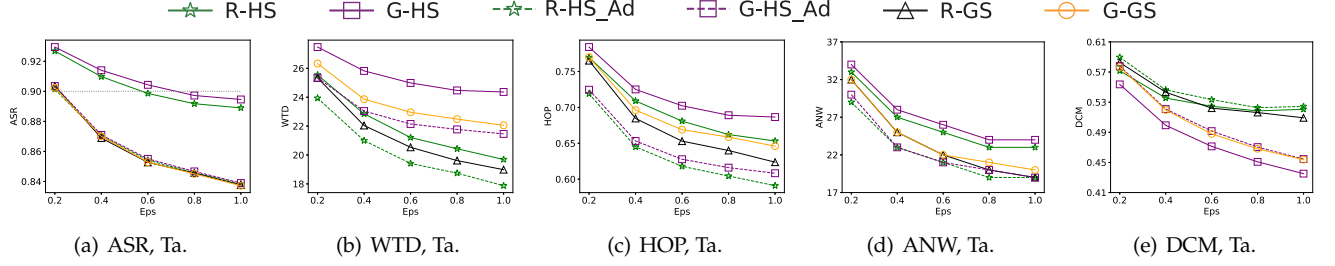


Fig. 5: Impact of application R on scheme performance

Algorithm 2 Finding *LGR***Input:** $R_0, D_{\min}, \text{task } t$ **Output:** R

- 1: c_t is the level-2 cell that covers t
- 2: R_0 is the distance between t and c_t
- 3: D_{\min} is half the width of the minimal cell
- 4: Compute c_t 's utility u
- 5: Init $U = u, R = R_0$
- 6: If $U \geq EU$, return R
- 7: $R = R + D_{\min}$
- 8: Add all cells in the R area to a set $\tilde{R} = \{c_1, c_2, \dots, c_n\}$
- 9: $\tilde{N} = \{N_1, N_2, \dots, N_n\}$ is the noisy worker count of \tilde{R}
- 10: $\bar{d} = \frac{\sum_{i=1}^n (\text{distance}(c_i, t) \times |N_i|)}{\sum_{i=1}^n |N_i|}$, \bar{d} is the average distance of workers to t in R area
- 11: $N_{\text{sum}} = \sum_{i=1}^n N_i$
- 12: The average AR in R area: $\overline{AR} = (1 - \bar{d}/MTD) \times MAR$
- 13: If $N_{\text{sum}} > 0$ then $U = 1 - (1 - \overline{AR})^{N_{\text{sum}}}$
- 14: Goto Line 6

series of experiments will demonstrate the advantages of parallel budgeting strategies for partitioning with historical data learning from multiple perspectives.

5.3 Break for Nonpositive Neighbor Case

As described in Section 5.1, adding noise will generate a large number of negative cells (count of workers is negative after adding noise) which do not contribute positive utility when adding to GR . For this, we set a kind of 'Breaking' strategy. Except for the initial cell where the task is located, when the next alternative cell to be added to the GR is a non-positive cell, the current GR will be returned directly, and the cell will not be added. We compared the 'Breaking' strategy on the Gowalla(Go.), and the results are shown in Figure 6.

It can be seen from the CELL index (number of cells in GR) in Figure 6 that after the 'Breaking' strategy is applied, the CELL is reduced by 1.0% without causing a significant decrease in ASR, indicating that the real utility contribution of the negative cell is not high on average. In terms of indexes, after applying the 'Breaking' strategy, the WTD and HOP have been reduced by about 0.4% and 0.3%, respectively.

5.4 Privacy Analysis

In this section, we focus on the analysis of privacy budget and protection in the whole system framework. The budget allocation is detailed shown in Figure 7.

Firstly, due to the totally different original data adopted at two stages, PSD stage and GR construction stage, one can allocate the full privacy budget ϵ in parallel composition according to the parallel combination theorem (theorem 2). That is, the privacy budget is assigned as ϵ in PSD stage and also ϵ in GR construction stage. This mechanism of privacy budget improves greatly the quality of the whole framework.

Secondly, at the PSD stage, we employ historical data and add Laplace noises at two levels for predictions. The privacy budget $\epsilon_1 = \beta\epsilon$ for Laplace noises added independently to the everyday count of workers in the whole domain (in the latest 20 days) are in parallel as well as the budget, $\epsilon_2 = (1 - \beta)\epsilon$, for the noise in each level-1 cell. This makes partitioning results independent of the real-time data. The partition between the two levels forms the sequence allocation of the privacy budget (theorem 1), which satisfies ϵ -DP protection.

Thirdly, in the GR construction stage, real-time data is imported into the partitioned grid, and Laplace noise of privacy budget ϵ is added to each level-2 cell, the privacy of real-time data is protected while the performance of the system is improved effectively.

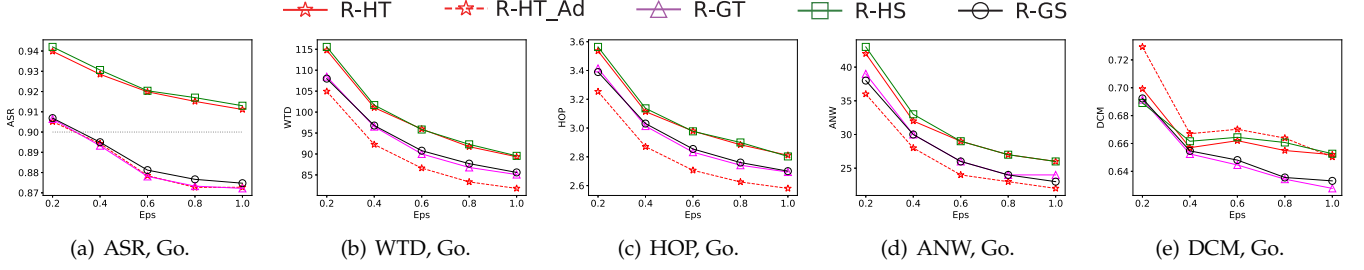


Fig. 6: Impact of application 'Breaking' on scheme performance

Finally, involving the learning of historical noisy data, 'Breaking' strategies and *LGR* operations and combined with the characteristics of post-processing (Theorem 3), the whole system scheme satisfies ϵ -DP protection.

6 PERFORMANCE EVALUATION

In this section, we mainly present an experimental evaluation of our R-HT scheme. In particular, we compare the system quality of R-HT with that of G-GR.

6.1 Experimental Methodology

Experimental comparison. Historical data learning technique has been shown to provide relatively high predictive accuracy [20, 21]. In order to verify the system quality of the proposed R-HT scheme, we carry out a series of experiments to compare it with the GDY [4], G-GR [6] and G-GS. Indeed, the G-GS scheme is modified from G-GR, where the utility rule is replaced by a newly designed scoring function for each grid cell selection.

Selection of Datasets. We use three real datasets: NYTaxi (NYC's Taxi Trip Data), Gowalla and Yelp.

NYTaxi is a New York taxi location dataset. We collected taxi pickup positions in New York City for 21 days from May 1 to May 21, 2013. The first 20 days are used as historical data, and 27,165 positions on May 21 are used as real-time data. The pickup position is modeled as the workers' position in *spatial crowdsourcing* (SC). Since most of the taxi pickup positions are distributed on the city's main roads, in order to better simulate the actual position of the workers, we randomly and uniformly blur each position into a circle with the current position as the center and the radius (*Blur Radius*, *BR*) of 80 m.

Gowalla is a social network check-in dataset. We extracted the check-in locations for 42 days from September 5 to October 16, 2010. Due to the large geographic span of the data, we adopted a simulation method to reduce the geographical distance by a ratio of 280 : 1. The data was merged into 1 time period every 2 days, and the last period was 6,736 location points for real-time data. Each restaurant location is modeled as the workers' position in SC, *BR* is 250 m.

Yelp corresponds to the data of the Phoenix area of Arizona. We have taken location data from March 2014 to August 2017. The data was merged into 1 time period every 2 months, the last period was used as real-time data, a total of 17,730 locations. We modeled the location of each restaurant as the workers' position in SC, *BR* is 600 m.

TABLE 2: Parameters of Datasets

Name	Historical Locations	Real-time Workers	MTD/m	Tasks
NYTaxi (Ta.)	841080	27165	300	2000
Gowalla (Go.)	133771	6736	1200	
Yelp (Ye.)	363330	17730	3000	

We can set scenes for the above three datasets respectively. For example, NYTaxi can be regarded as a taxi ordering scene in the downtown area. The maximum distance for taxi drivers to take orders is 500 m. *MTD* is 90% of *MCD* which is determined according to Eq. (7), calculated in 300 m. Considering Gowalla as a takeaway booking scenario, the maximum order distance is 2 km, and the *MTD* is calculated to be 1.2 km. Yelp is considered to be a car repair scenario. The maximum order distance is 5 km, so *MTD* is 3 km. At the same time, 2,000 positions are randomly and evenly selected from the workers' positions as task points. The relevant parameters of the dataset are shown in Table 2.

In our experimental settings, privacy budget $\epsilon \in \{0.2, 0.4, 0.6, 0.8, 1.0\}$, expected utility $EU \in \{0.6, 0.7, 0.8, 0.9\}$, and maximum task acceptance probability $MAR \in \{0.05, 0.1, 0.15, 0.2, 0.25\}$. Where the default values for ϵ , EU and MAR are set to 0.5, 0.9 and 0.1, respectively.

The utility loss caused by DP can be seen more intuitively by setting a non-privacy scheme, which constructs *GR* by selecting workers closest to the task one by one within the *MTD* region. The HOP value of *GR* is calculated based on the distance between the two farthest workers. In GDY and G-GR, in order to avoid the influence of the

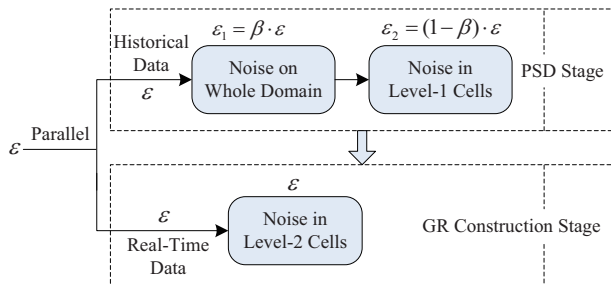
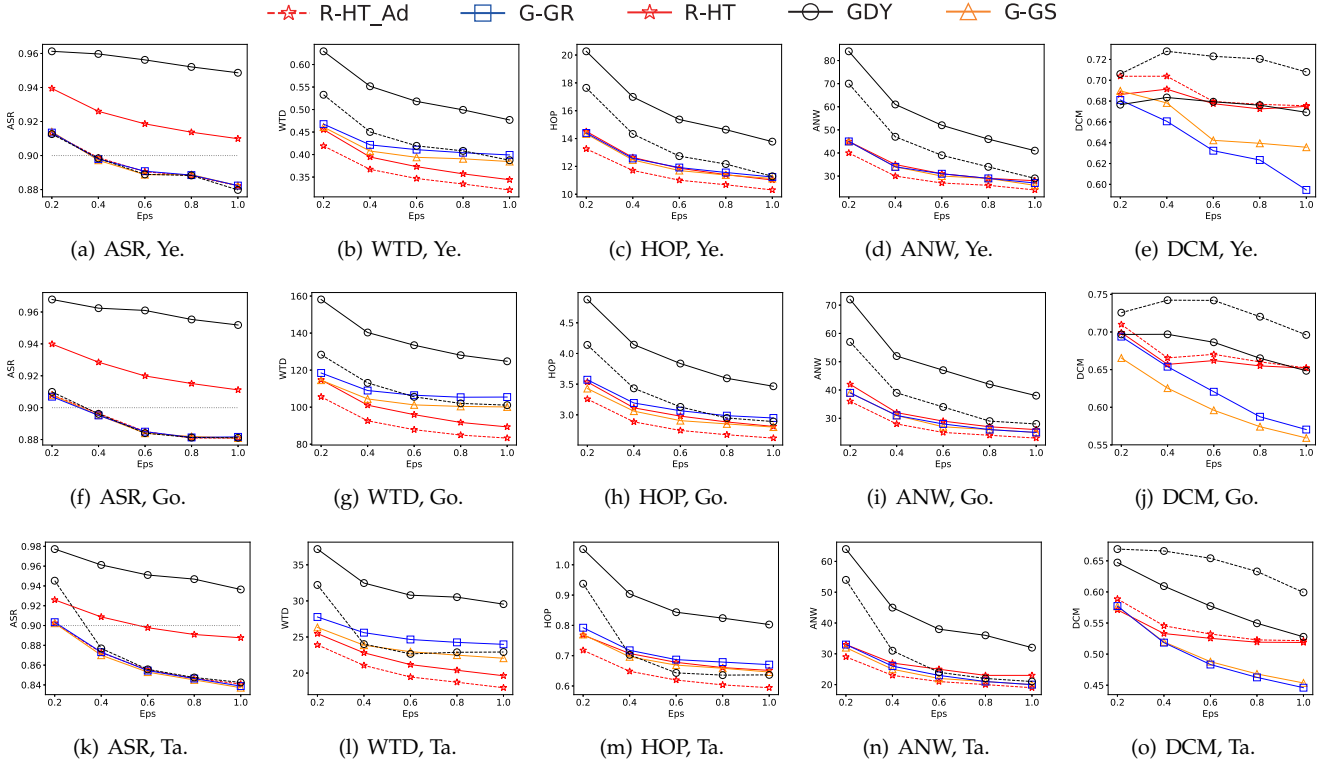


Fig. 7: Privacy budget allocation

Fig. 8: Comparison on GR indexes by varying ϵ

randomness of noise on grid partition, we cycle the whole process 50 times to get 50 groups of results, and extract the average value of indexes. In the R-HT, the process of adding noise during grid partition is executed 5 times to obtain 5 groups of partition results. The real-time data in the level-2 cells in each group is added noise randomly with 20 times, a total of 100 groups of population distribution map with grid. For all schemes, 2000 single-task-assignments are performed on each map, regardless of the allocation conflicts between each task in space and time, so as to obtain stable results of performance evaluation of each scheme under this scenario (single task and single worker). Next, we investigate the effects of varying privacy budget, MAR and expected utility, respectively, and also evaluate LGR -Based Heuristics and the running time of the schemes for feasibility.

6.2 Task Allocation Evaluation

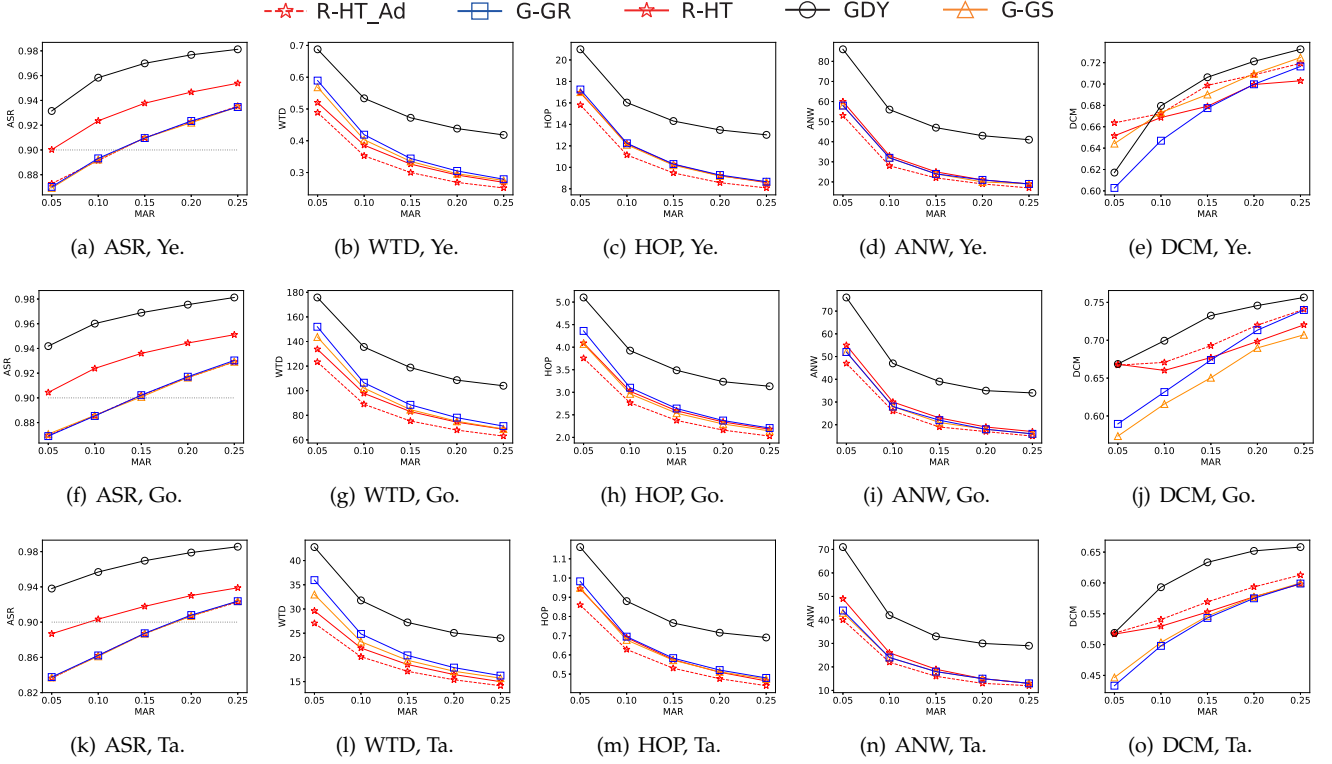
In this section, we evaluate the performance of R-HT and other related schemes on three datasets by using different parameters (privacy budget ϵ , maximal acceptance rate MAR and expected utility EU). Performance is measured by the five main indicators presented in Section 4.4 and the CELL indicators (the number of grids in GR)

6.2.1 Effect of Varying Privacy Budget

We start by focusing on the impact and comparison of the major schemes of the changes to the privacy budget, as Figure 8. With the increase of privacy budget, the ASR of each scheme decreases gradually, which is mainly related to the partition granularity. When the privacy budget is low, in order to resist the noise, the granularity increases

caused more larger cells, so there is a significant oversupply when adding the last cell to GR . When the default $EU=0.9$ is used uniformly, ASR of R-HT can basically reach the threshold, while G-GR fails in most cases. On this basis, R-HT is 10.4%, 1.8% and 6.7% better than G-GR on average on WTD, HOP and DCM, with a maximum increase of 13.3%, 2.8% and 7.2% respectively. This shows that R-HT can basically ensure the task acceptance probability to reach EU , and also achieve better results than G-GR in all indexes. Because the use of historical data reduces the loss caused by adding noise, and then brings more appropriate adaptive grid partition and grid selection with higher density of actual population and closer distance. The ASR of R-HT in NYTaxi is relatively low, because a small MTD causes AR decreasing rapidly with the increase of distance, the number of cells GR needed will be a little large, which brings a larger virtual number of workers, and the real ASR will be lower.

By adjusting EU to R-HT and GDY, the ASR of each scheme is approximately the same, and the advantage of R-HT_Ad is more obvious. Compared with G-GR, the average decrease of HOP in R-HT_Ad and G-GS is 9.3% and 2.9%, respectively. Especially in NYTaxi, the decrease of HOP in R-HT_Ad is 10.2%. This is because using scoring function involved area and distance, both R-HT_Ad and G-GS prefer to choose cells with high distribution density or closer distance. R-HT_Ad has the most obvious advantage in WTD, with an average reduction of 17.1% in three datasets. In ANW, R-HT_Ad reduced the number of workers by 9.7% compared with G-GR. In addition, we can see the change of DCM, GDY has the best effect all the time, which is also well understood, GDY has the coarsest partition granularity results in the smallest number of selected cells, and even

Fig. 9: Comparison on GR indexes by varying MAR

it's enough to only publishes one grid where the task is located. The DCM of R-HT_Ad is 8.1% higher than that of G-GR because of the addition of LGR strategy. To sum up, within the range of dramatic changes in the privacy budget, R-HT can not only basically meet EU , but also effectively reduce the actual cost of workers accepting tasks, and also improve the compactness of GR , thus effectively saving communication costs and improving system operation efficiency comprehensively.

6.2.2 Effect of Varying MAR

We observed the indexes change and correlation comparison of R-HT by changing MAR , as Figure 9. The results show that the increase of MAR will reduce the HOP and WTD, because it will increase AR, so that fewer workers nearby may enough meet the requirements of EU . At the same time, influenced by the change of MAR , the decrease of HOP and WTD is faster as well as the decrease of cells' number needed in GR which is more obvious than the impact of EU changes. Except for a few points, the ASR of the R-HT has all met EU , while the ASR of the G-GR has nearly half of them failed. Compared with the G-GR, the maximum improvement of the WTD, HOP, ANW and DCM of the R-HT_Ad are 18.7%, 10.9%, 9.0% and 7.0%, respectively.

6.2.3 Effect of Varying EU

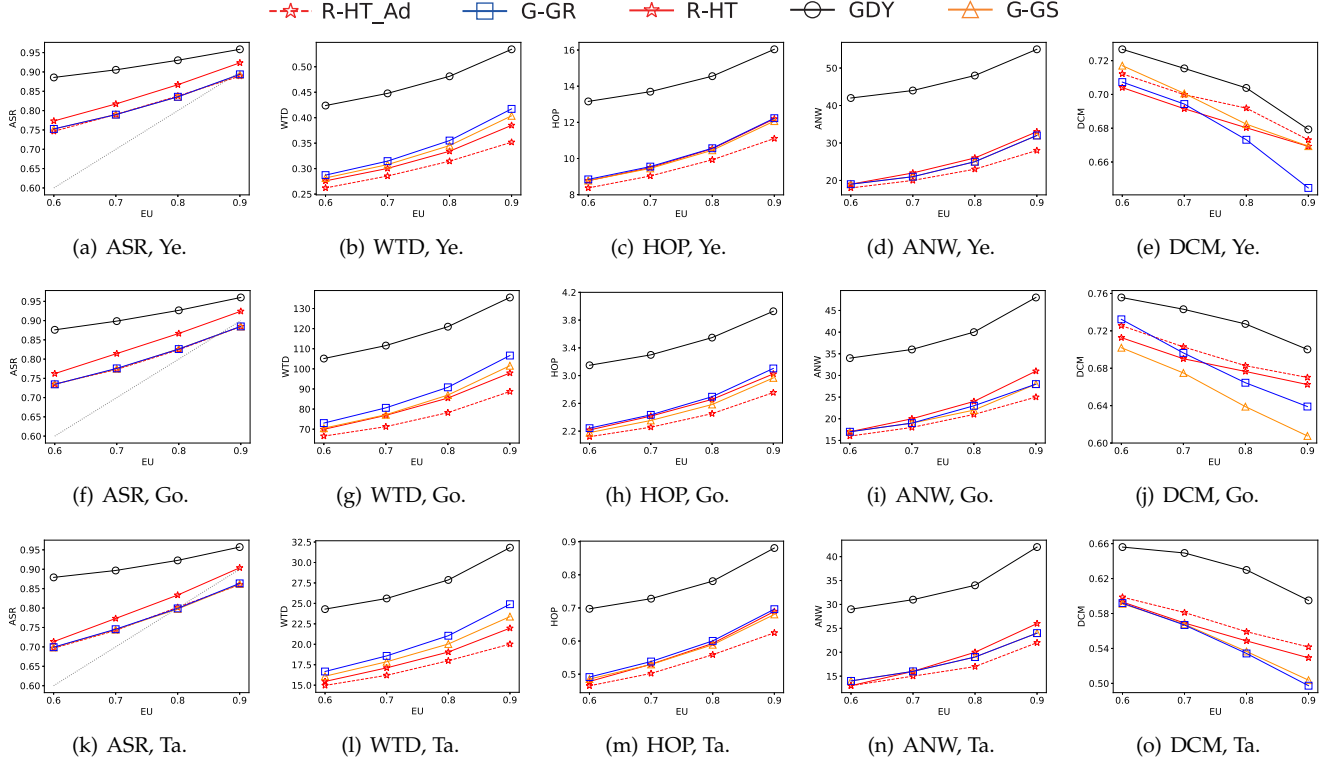
We observed the influence of EU changes on the indexes of R-HT and other schemes and made comparative analysis. Obviously, when EU increases, the GR area will increase, so both WTD and HOP will increase. Experiments show that under different EU s, all ASR of R-HT meet the threshold

and the WTD and HOP are always smaller than those of G-GR. With the increase of EU , the more cells are selected, and the more obvious this gap is. When EU equals 0.9, the gaps between R-HT_Ad and G-GR on WTD, HOP, ANW and DCM are up to 19.6%, 11.2%, 12.5% and 8.9%, respectively.

According to the ASR results of the above three experiments (sections 6.2.1 to 6.2.3), the R-HT basically reached EU under various parameter settings. In most cases, the G-GR failed to reach EU , and relevant statements can be referred to Section 7.2.1 of [6]. Therefore, G-GR doesn't address the challenge of achieving a high success rate for the task assignment. In the specific experimental results, a total of 42 groups of ASR values were compared under different combinations of parameters ϵ , EU and MAR on three datasets. Among them, 19 points of G-GR reached EU , accounting for 45.2%, while 38 points of R-HT reached EU , accounting for 90.5%, twice as much as G-GR. We analyzed the compliance rates of ASR on Yelp, Gowalla and NYTaxi, G-GR was 50.0%, 50.0% and 35.7% and R-HT was 100.0%, 100.0% and 71.4%, respectively. Both of the two schemes have some standard percentage gaps in NYTaxi. This is because the MTD of NYTaxi is small, the AR decreases rapidly with the increase of distance, the number of cells GR needed will be a little large, which brings a large vitural number of workers causes ASR decreasing.

6.3 Evaluation of LGR-Based Heuristics

The experiment found that the use of the LGR strategy will improve the effect of R-HT, but in the experiments we found that the calculated local radius R is often too large. Through analysis, in the GR construction stage, the proportion that the whole LGR is still no enough for EU , adopt 1.0R (0.0%),

Fig. 10: Comparison on *GR* indexes by varying *EU*

0.9R (2.1%) and 0.88R (4.3%), the proportion is lower. So we compared 0.9R and 0.88R to the improved hybrid scheme of the G-GR, the experimental results running on the Gowalla are shown in Figure 11.

When local radius R is reduced, the ASR of the R-HT will decrease naturally. This is because the reduction of R will reduce the range of cell selection caused smaller cells in *GR*. When R is reduced to 0.88 times, most points of the ASR on the Gowalla can still reach *EU*. The adoption of the G-GR_hybrid scheme did not significantly affect the ASR of G-GR on the Gowalla. 0.88R-HT has a clear advantage in WTD, on average it is 12.4% smaller than G-GR_hybrid. On HOP, although the two schemes are entangled, 0.88R-HT still keeps a 0.4% advantage overall. On the ANW, 0.88R-HT is higher since the higher ASR. But on DCM, 0.88R-HT gradually changed from advantage to disadvantage, which is mainly related to the utility function (Eq. (12)) of G-GR_hybrid.

$$U_t^s = (1 - \epsilon) \times u \times (1 - \alpha) + \epsilon \times \text{Comp} \times \alpha \quad (12)$$

$\alpha = 0.3$, u represents the task acceptance probability of the cell s , and Comp represents the DCM of *GR* after s is added to *GR*. As ϵ increases, the DCM weight in the utility function becomes larger. When ϵ is equal to 1.0, at this time, the utility function is only related to DCM.

Comparing non-privacy situation, we can observe that non-privacy has obvious advantages in WTD and HOP because it is not partitioned into grids. On ANW, we can see that 0.88R-HT, G-GR and G-GR_hybrid are closer to the non-privacy scheme when ϵ equals 1.0, indicating that the three schemes have played a better role in reducing ANW, but the ASR of 0.88R-HT is higher at this time.

In addition, To et al [6] proposed a partial cell selection based on G-GR to deal with the ASR overflow problem when the last cell is added to *GR*, so as to reduce the system overhead to some extent. However, under the severe challenge that the actual ASR fails to reach *EU*, the partial cell selection will undoubtedly aggravate this trouble, which has been demonstrated by our experiments. Therefore, in this paper, the additional partial strategy in R-HT is not considered.

6.4 Test on Running Time

In real life, besides the task assignment success rate and communication cost, the time from request to release is also very important for the assignment of tasks. We divided the entire assignment process of a single task into two major stages. The first stage is the grid partition (stage A), which includes the grid partition and adding noise to the number of real-time workers. When using historical data, this stage can be divided into the following two stages: First, partitioning grid with noisy historical data (stage A1); Then, updating real-time data and adding noise to the count of workers in level-2 cells (stage A2). The second stage is the *GR* construction stage (stage B).

We consider the following three comparisons in terms of time consuming: First, the entire process (A+B), which represents the running time of the entire algorithm; Second, updating real-time data and constructing *GR* (A2+B) after grid partition with historical data which is applicable to scenarios where the real-time data changes greatly in a period of time and we need update real-time data before constructing *GR*; Third, constructing *GR* after updating real-time data. We used Python 2.7 on Windows 10 (2.4GHZ

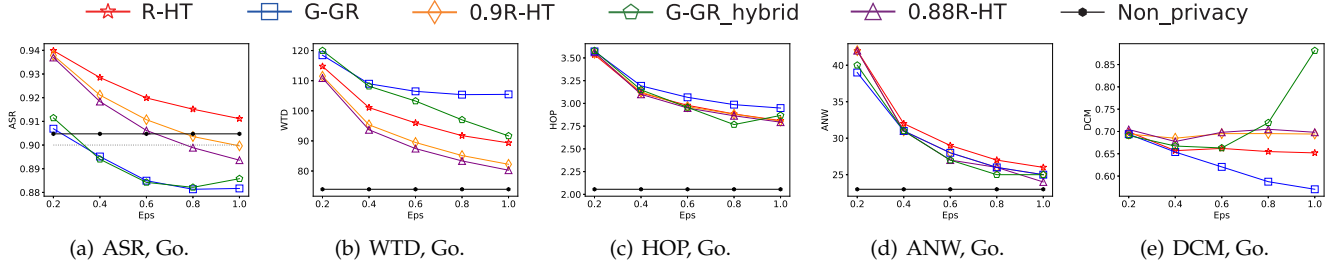


Fig. 11: Comparison between R-HT with different R and G-GR_hybrid on Gowalla

Intel i5 CPU, 8G RAM) to run 2,000 tasks on three datasets, and calculated each time consumption in 10 cycles, taking the average as the time result, as shown in the Table 3.

TABLE 3: Time Consuming of R-HT and G-GR Over Three Datasets

Stage	Yelp (workers' count: 363330 + 17730)		Gowalla (workers' count: 133771 + 6736)		NYTaxi (workers' count: 841080 + 27165)	
	R-HT	G-GR	R-HT	G-GR	R-HT	G-GR
B	20.4 ms	0.5 ms	9.8 ms	0.5 ms	16.9 ms	0.6 ms
A2+B	21.3 ms	\	10.1 ms	\	17.5 ms	\
A+B	1.56 s	62 ms	0.5 s	22 ms	2.84 s	0.1 s

It can be seen from the results in the table that in stage B, R-HT takes a long time, because R-HT needs to calculate R , and not only need calculate cell's utility but also cell's score. For stage A2+B, compared with stage B, it can be seen that updating data and adding noise only take a very small period of time (less than 1ms), and there is no data update in G-GR after grid partition. In stage A+B, we can see that the time consumption in grid partition is far greater than the time consumption in GR construction, mainly in the process of historical data prediction, which increases the time consumption in R-HT. The running time of a single task on the three datasets is controlled within 3s, which forms an approximate direct proportion with the total count of real-time data, which can guarantee the timeliness and practicability of task release in real life.

7 CONCLUSION

In this paper, we proposed a location protection model for worker dataset in SC based on DP, which ensures that the privacy of worker locations is not disclosed at the task allocation stage. We first introduced historical data learning into domain partitioning and then we achieved parallel use of privacy budget. This significantly reduces scales of random noises and enables the real ASR to reach the expected utility threshold stably. Moreover, We proposed several optimization techniques for constructing GR . Our experimental results on real data demonstrated that the proposed R-HT scheme reduces the system overhead, and the time cost is practical.

Currently, we analyze a single-task (single-worker only) framework for privacy protection worker locations based on historical data learning. If there is only real-time data,

data segmentation (one part for domain partitioning and the other for GR construction) can also achieve parallel composition of privacy budget. This situation will be discussed in a forthcoming paper. As future work, we aim to extend the privacy framework for the scenario of multi-task parallel assignments in SC and explore new cell selection strategies.

REFERENCES

- [1] H. To and C. Shahabi, *Location Privacy in Spatial Crowdsourcing*, A. Gkoulalas-Divanis and C. Bettini, Eds. Cham: Springer, 2018.
- [2] Y. Tong, Z. Zhou, Y. Zeng, L. Chen, and C. Shahabi, "Spatial crowdsourcing: A survey," *The VLDB Journal*, vol. 29, no. 1, pp. 217–250, 2020.
- [3] Y. Xiao, L. Xiong, and C. Yuan, "Differentially private data release through multidimensional partitioning," in *Workshop on Secure Data Management*. Springer, 2010, pp. 150–168.
- [4] W. Qardaji, W. Yang, and N. Li, "Differentially private grids for geospatial data," in *2013 IEEE 29th International Conference on Data Engineering (ICDE)*. IEEE, 2013, pp. 757–768.
- [5] H. To, G. Ghinita, and C. Shahabi, "A framework for protecting worker location privacy in spatial crowdsourcing," *Proceedings of the VLDB Endowment*, vol. 7, no. 10, pp. 919–930, 2014.
- [6] H. To, G. Ghinita, L. Fan, and C. Shahabi, "Differentially private location protection for worker datasets in spatial crowdsourcing," *IEEE Transactions on Mobile Computing*, vol. 16, no. 4, pp. 934–949, 2017.
- [7] X. Wang, Z. Liu, X. Tian, X. Gan, Y. Guan, and X. Wang, "Incentivizing crowdsensing with location-privacy preserving," *IEEE Transactions on Wireless Communications*, vol. 16, no. 10, pp. 6940–6952, 2017.
- [8] C. Yin, J. Xi, R. Sun, and J. Wang, "Location privacy protection based on differential privacy strategy for big data in industrial internet of things," *IEEE Transactions on Industrial Informatics*, vol. 14, no. 8, pp. 3628–3636, 2017.
- [9] T. Zhu, G. Li, W. Zhou, and S. Y. Philip, *Differential Privacy and Applications*. Springer, 2017, vol. 69.
- [10] R. Shokri, G. Theodorakopoulos, C. Troncoso, J. P. Hubaux, and J. Y. Le Boudec, "Protecting location privacy: Optimal strategy against localization attacks," in *Proceedings of the 2012 ACM Conference on Computer and Communications Security*, 2012, pp. 617–627.
- [11] M. E. Andrés, N. E. Bordenabe, K. Chatzikokolakis, and C. Palamidessi, "Geo-indistinguishability: Differential

- privacy for location-based systems," in *Proceedings of the 2013 ACM SIGSAC Conference on Computer & Communications Security*, 2013, pp. 901–914.
- [12] B. Liu, L. Chen, X. Zhu, Y. Zhang, C. Zhang, and W. Qiu, "Protecting location privacy in spatial crowdsourcing using encrypted data," *Advances in Database Technology-EDBT*, pp. 478–481, 2017.
- [13] P. Xiong, L. Zhang, and T. Zhu, "Reward-based spatial crowdsourcing with differential privacy preservation," *Enterprise Information Systems*, vol. 11, no. 10, pp. 1500–1517, 2017.
- [14] H. To, C. Shahabi, and L. Xiong, "Privacy-preserving online task assignment in spatial crowdsourcing with untrusted server," in *2018 IEEE 34th International Conference on Data Engineering (ICDE)*. IEEE, 2018, pp. 833–844.
- [15] Z. Wang, X. Pang, Y. Chen, H. Shao, Q. Wang, L. Wu, H. Chen, and H. Qi, "Privacy-preserving crowdsourced statistical data publishing with an untrusted server," *IEEE Transactions on Mobile Computing*, vol. 18, no. 6, pp. 1356–1367, 2018.
- [16] J. Wei, Y. Lin, X. Yao, and J. Zhang, "Differential privacy-based location protection in spatial crowdsourcing," *IEEE Transactions on Services Computing*, 2019.
- [17] X. Li, Y. Wang, X. Zhang, K. Zhou, and C. Li, "A more secure spatial decompositions algorithm via infeasible laplace noise in differential privacy," in *International Conference on Advanced Data Mining and Applications*. Springer, 2018, pp. 211–223.
- [18] Y. Gong, C. Zhang, Y. Fang, and J. Sun, "Protecting location privacy for task allocation in ad hoc mobile cloud computing," *IEEE Transactions on Emerging Topics in Computing*, vol. 6, no. 1, pp. 110–121, 2015.
- [19] D. Xu, Y. Wang, L. Jia, Y. Qin, and H. Dong, "Real-time road traffic state prediction based on ARIMA and Kalman filter," *Frontiers of Information Technology & Electronic Engineering*, vol. 18, no. 2, pp. 287–302, 2017.
- [20] R. Liu, G. Cong, B. Zheng, K. Zheng, and H. Su, "Location prediction in social networks," in *Asia-Pacific Web (APWeb) and Web-Age Information Management (WAIM) Joint International Conference on Web and Big Data*. Springer, 2018, pp. 151–165.
- [21] Y. Jiang, W. He, L. Cui, and Q. Yang, "User location prediction in mobile crowdsourcing services," in *International Conference on Service-Oriented Computing*. Springer, 2018, pp. 515–523.
- [22] Z. Chen, X. Kan, S. Zhang, L. Chen, Y. Xu, and H. Zhong, "Differentially private aggregated mobility data publication using moving characteristics," *arXiv preprint arXiv:1908.03715*, 2019.
- [23] L. Kazemi and C. Shahabi, "Geocrowd: Enabling query answering with spatial crowdsourcing," in *Proceedings of the 20th International Conference on Advances in Geographic Information Systems*, 2012, pp. 189–198.
- [24] L. Kazemi, C. Shahabi, and L. Chen, "Geotrucrowd: Trustworthy query answering with spatial crowdsourcing," in *Proceedings of the 21st ACM Sigspatial International Conference on Advances in Geographic Information Systems*, 2013, pp. 314–323.
- [25] X. Zhang, Z. Yang, Y. Liu, and S. Tang, "On reliable task assignment for spatial crowdsourcing," *IEEE Transactions on Emerging Topics in Computing*, vol. 7, no. 1, pp. 174–186, 2016.
- [26] C. Dwork, "Differential privacy," in *Proceedings of the 33rd International Conference on Automata, Languages and Programming - Volume Part II*, 06 2006, pp. 1–12.
- [27] C. Dwork and A. Roth, "The algorithmic foundations of differential privacy," *Foundations and Trends® in Theoretical Computer Science*, vol. 9, no. 3–4, pp. 211–407, 2014.
- [28] N. Li, M. Lyu, D. Su, and W. Yang, *Differential Privacy: From Theory to Practice*. Morgan & Claypool Publishers, 2016, vol. 8, no. 4.
- [29] B. J. Hecht and D. Gergle, "On the 'localness' of user-generated content," in *Proceedings of the 2010 ACM Conference on Computer Supported Cooperative Work*, 2010, pp. 229–232.
- [30] M. Musthag and D. Ganesan, "Labor dynamics in a mobile micro-task market," in *Proceedings of the SIGCHI Conference on Human Factors in Computing Systems*, 2013, pp. 641–650.